CHAPTER 3

GROWTH AND CHARACTERIZATION OF SODIUM PENTABORATE SINGLE CRYSTALS

3.1 INTRODUCTION

Extensive studies have been performed on borates due to their attractive physical and chemical properties such as piezoelectricity ($Li_2B_4O_7$), fast ionic conductivity ($Li_3B_5O_8$ $(OH)_2$), ion exchange capacity ($Na_2Co_2B_{12}O_{21}$), catalytic activity ($Cu_2Al_6B_4O_{11}$), charge ordering (Fe_2OBO_3) and the 'spin gap' behavior in the two dimensional frustrated antiferromagnetic $SrCu_2$ $(BO_3)_2$ (Zhen-Tao Yu et al 2003). These borate crystals generally possess chemical stability as well as wide range of optical transparency far into the ultraviolet on account of the rather large difference in the electronegativities of B and O atoms (Chuangtian Chen et al 1990). Moreover boron is unique because of its valence shell orbitals and vacant π orbitals, and planar ionic groups such as BO_3^{3-}, $B_3O_6^{3-}$ and $B_3O_7^{5-}$ which show interesting π-conjugation (Xia 1994).

The study of dielectric properties such as dielectric constant, dielectric loss and ac conductivity over a range of frequencies and temperatures help in assessing their electrical properties. The practical application of the anhydrous borate single crystals is seriously inhibited by the problem of superposition of necessary set of parameters for device fabrication and the difficulty in growing borate single crystals with device quality and size. It is known that for the growth of single crystals from

majority of perspective borates, it is necessary to use complex and long lasting methods, in particular, the high temperature solution top-seeding method (Adamiv et al 2006).

In this chapter, the growth of single crystals of sodium pentaborate $Na(H_4B_5O_{10})$ (SPB) by low temperature solution growth technique (slow evaporation solution growth) is reported for the first time in the literature. Highly transparent optical quality single crystals were grown within a growth period of 40 days. The grown single crystal was subjected to single crystal X-ray diffraction studies and the lattice parameters were obtained. Powder X-ray diffraction studies were also carried out for the grown crystal. The structural perfection of the grown NaB5 was analyzed by HRXRD study. The optical properties of the grown crystal were studied using the UV-Vis. and PL studies. The functional groups of the grown material were identified by FT-IR studies. The theoretical calculation of the vibrational modes in the crystal was carried out using the factor group analysis. The thermal and mechanical properties of SPB were studied using TG-DTA and Vickers microhardness tester respectively. The dielectric properties of the crystals were carried out to explore the electrical properties of the crystal.

3.2 GROWTH OF SODIUM PENTABORATE SINGLE CRYSTALS

3.2.1 Material Synthesis

Sodium pentaborate, $Na(H_4B_5O_{10})$ was synthesized by reacting commercially available boric acid and sodium carbonate (99.9%) 10:1 molar ratio using deionized water as solvent. The reaction is as follows:

$$Na_2CO_3 + 10H_3BO_3 \rightarrow 2[Na(H_4B_5O_{10})\ 2H_2O] + 7H_2O + CO_2\uparrow$$

The synthesized salt of SPB was subjected to repeated recrystallization process in order to increase the purity of the crystal using deionized water as the solvent.

3.2.2 Solubility

Solubility is the characteristic physical property referring to the ability for a given substance to dissolve in the appropriate solvent. The solvent can directly affect the crystal growth through its influence on the desolvation process. This can have a significant impact on the crystal size, morphology and purity of the crystal. The solubility test gives a key to select the best solvent and temperature to grow good quality single crystals. Solubility of NaB5 in deionized water was determined at different temperatures (35˚C to 60˚C) before incepting the crystal growth process. The NaB5 solution was prepared using deionized water as solvent at a required temperature with continuous stirring to ensure homogeneous temperature and concentration over the entire volume of the solution. On reaching saturation, the content of the solution was gravimetrically analyzed. Figure 3.1 shows the solubility of NaB5 in deionized water at various temperatures. It is observed from the graph that solubility increases with increase in temperature and hence sodium pentaborate (SPB) exhibits a positive solubility temperature gradient in deionized water.

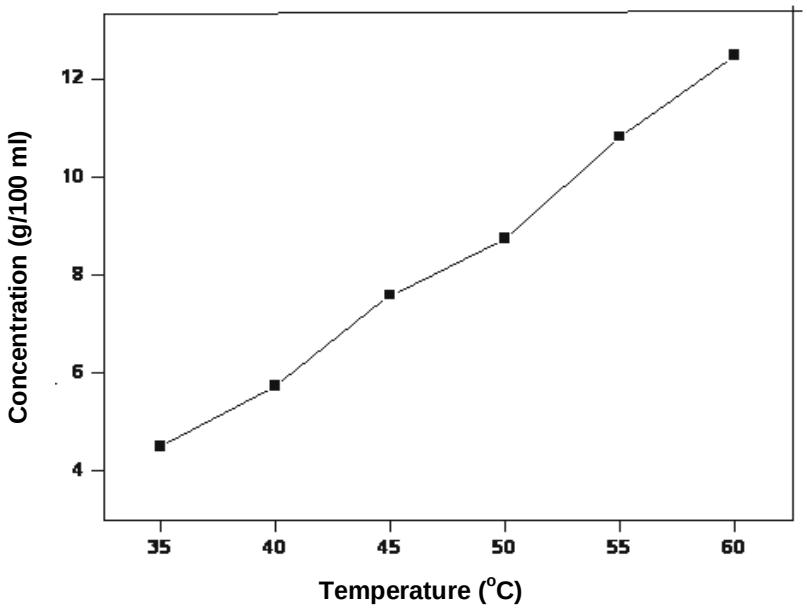

Figure 3.1 Solubility curve of sodium pentaborate

3.2.3 Growth of Sodium Pentaborate (SPB) Crystals

Among the various crystal growth methods employed for the growth of bulk size crystals, solution growth method is the simplest and mostly used (Brice 1986) than the other methods just for the reason that it has less sophisticated instrumentation and ease of handling. Moreover, crystals of different orientations and morphology can be grown from this method. Hence to grow the single crystals of SPB, slow evaporation solution growth method was employed. The supersaturated solution of SPB was prepared at 40^{o}C using deionized water and the beaker containing the solution was housed in the constant temperature bath (accuracy ±0.01°C) for controlled evaporation. Good quality single crystals were obtained after 40 days with well defined morphology and the grown crystals are shown in Figure 3.2.

Figure 3.2 As grown crystals of sodium pentaborate

3.3 STRUCTURAL CHARACTERIZATION OF SODIUM PENTABORATE (SPB) CRYSTALS

3.3.1 Single Crystal X-ray Diffraction Studies

The morphology and the cell dimensions of sodium pentaborate were identified by single crystal X-ray diffraction analysis using ENRAF NONIUS CAD 4 single crystal X-ray diffractometer. A crystal of dimensions $0.5 \times 0.6 \times 0.6$ mm^3 obtained from the grown bulk SPB was used as specimen for analysis. It is found from the single crystal X-ray diffraction analysis that SPB crystallizes in the monoclinic system with the space group $P2_1/c$ and the cell parameters are a = 11.103 Å, b = 16.437 Å and c = 13.564 Å with $\alpha = 89.96^o$, $\beta = 112.85^o$ and $\gamma = 89.96^o$. The morphology of the grown crystal and the prominent planes (010), (331) and (021) are shown in Figure 3.3. The summary of the crystal properties of SPB crystal is given in Table 3.1.

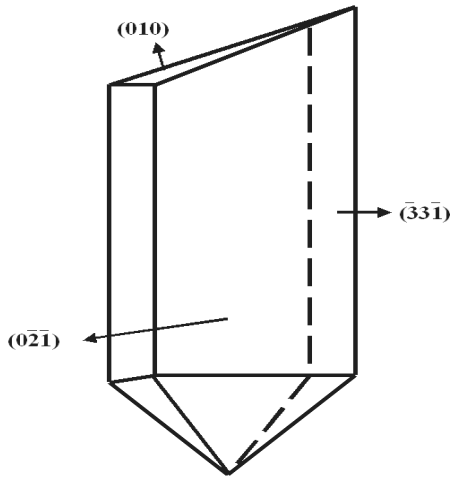

Figure 3.3 Morphology of sodium pentaborate

Table 3.1 Crystal Properties of SPB

Molecular formula	$Na[H_4B_5O_{10}]$
Molecular Weight	240
Crystal structure	Monoclinic
Space group	$P2_1/c$
Cell parameters	a = 11.103 Å b = 16.437 Å c = 13.564 Å α = 89.96° β = 112.85° γ = 89.96°
Volume	2280.7742 $Å^3$
No. of atoms per unit cell (Z)	4
Radiation	MoKα
Wavelength	0.71069 Å
Colour	Colourless
Hygroscopicity	Non- hygroscopic

3.3.2 High Resolution X-Ray Diffraction Studies on SPB Crystal

In the last two decades semiconductor industries are analyzing the generation of defects in the grown crystals using HRXRD studies because the information about the crystalline quality can be readily obtained, which is then rapidly fed back to crystal growth laboratories. There are many reports existing with respect to high resolution X-ray diffraction studies on inorganic crystals (Anantha Murthy et al 1993 and Sato et al 2003). The grown single crystal of SPB was subjected to HRXRD studies using the setup described in section 2.3.2.

Figure 3.4 shows the high resolution X-ray diffraction curve (rocking curve) recorded with multicrystal X-ray diffractometer using (131) diffracting planes for SPB single crystal. The diffraction curve contains only a single peak and is quite sharp with full width at half maximum (FWHM) of 20 arc sec. The absence of additional peaks and very low FWHM indicate that the specimen crystal does not contain any internal structural grain boundaries and the crystalline perfection of SPB is very good.

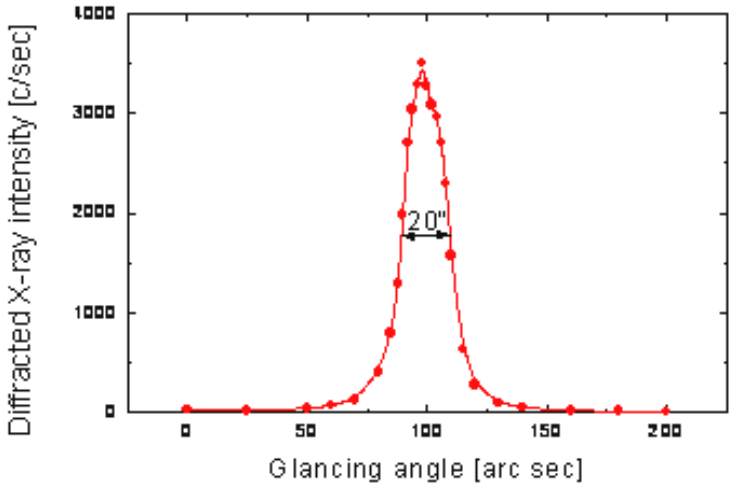

Figure 3.4 High resolution X-ray diffraction curve of SPB single crystal

3.3.3 Photoluminescence Studies

The photoluminescence spectroscopy is a nondestructive method of testing used to study in detail the electronic structure of materials. The PL spectrum of the SPB crystal is shown in Figure 3.5. This shows a broad band at 559 nm. The intensity of the peak is low for SPB crystal. The strong yellow emission peak is observed at 559 nm corresponding to the energy of 2.22 eV. As $Zn_2(OH)BO_3$ exhibits similar visible emission at 559 nm, the nature of these yellow bands at 2.3eV and 2.2eV can be attributed to radiative recombination between deep donors and shallow acceptors (Meijerink et al 1990). The absence of the additional peaks reveals the high structural perfection of the grown SPB crystals, which can also be inferred from the HRXRD spectrum shown in Figure 3.4.

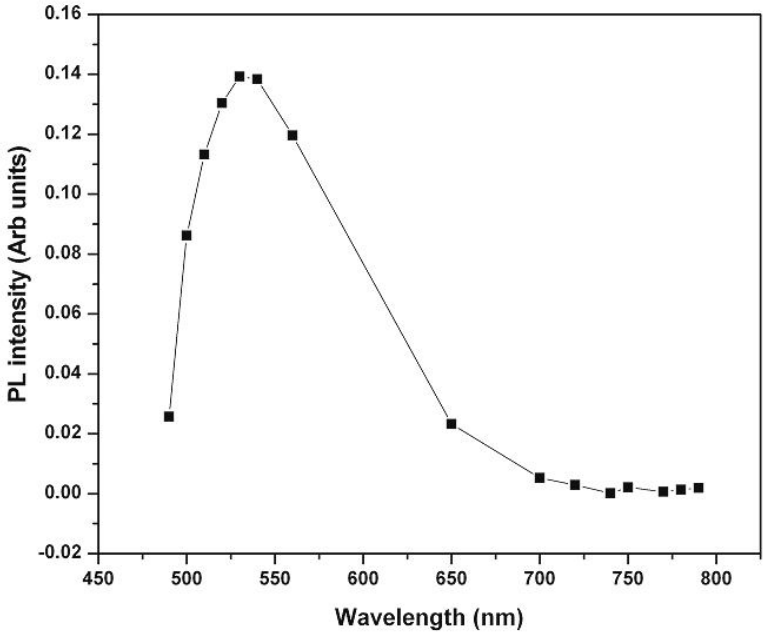

Figure 3.5 Photoluminescence spectrum of sodium pentaborate (SPB)

3.3.4 Spectral Analyses

3.3.4.1 Factor group analysis

The vibrational spectroscopy is an important tool in understanding the chemical bonding and provides useful information in studying the microscopic mechanism of the new crystals that are generated. The site group and the factor group are important in group theoretical methods for the analysis of spectra of solids. Also the factor group method provides a basis for the prediction of theoretical IR and Raman spectra of lattice vibrations. The single crystal X-ray diffraction studies performed for the SPB crystal confirms that the SPB crystal belongs to the monoclinic crystal system with the space group of $P2_1/c$. There are totally 4 atoms per unit cell, which occupies the general sites of $C_1(4)$ symmetry. There are 20 atoms in a single molecule of SPB which in turn gives rise to (20×4) 80 atoms in a unit cell. Group theoretical analysis of the fundamental modes of SPB crystal predicts that there are 240 vibrational optical modes and are seen to decompose into $\Gamma_{237} = (60A_g + 59\ A_u + 60\ B_g + 58\ B_u)$ apart from three acoustic modes $(1A_u + 2\ B_u)$. The factor group analysis for SPB crystal was performed by following the procedures outlined by Rousseau et al (1981). The summary of the factor group analysis of SPB is given in Table 3.2.

3.3.4.1.1 Vibrational analysis of SPB

The vibrational analysis of SPB reveals the structures of the co-ordinated compounds, information on the nature of bonding and the confirmation of the material. The calculated vibrations of SPB could be due to lattice vibrations and internal vibrations of the co-ordinated compounds mostly the B-O and O-H groups. The formal calculation of fundamental modes of SPB reveals 216 internal vibrations which can be attributed as $(54A_g + 54\ A_u + 54\ B_g + 54\ B_u)$ and 24 external modes contributed by

9 translational and 12 rotational modes. The bands observed between 4000 to 500 cm^{-1} is due to the internal vibrations of the co-ordinated compounds and the peaks below 500 cm^{-1} arise from the deformational vibrations and the translational and rotational modes of the compounds. The internal modes of SPB ions split into four components of which all are IR active and A_g (XX,YY, ZZ, XY) and B_g (XZ,YZ) are Raman active.

Table 3.2 Factor group analysis summary of SPB

Factor group species	Site Symmetry (C_1(4))		Na	B	O	H	Optical modes	Acoustic modes	Total
	Internal	External							
A_g	54	3T, 3R	3	15	30	12	60	0	60
A_u	54	3T, 3R	3	15	30	12	60	1	59
B_g	54	2T, 3R	3	15	30	12	60	0	60
B_u	54	1T, 3R	3	15	30	12	60	2	58
Total	**216**	**9T, 12R**	**12**	**60**	**120**	**48**	**240**	**3**	**237**

3.3.4.1.2 Internal vibrations

The internal vibrations of SPB are those arising from the B-O symmetric and asymmetric stretching bonding and the O-H stretch of $[B_5O_6(OH)_4]$ modes of vibrations.

In SPB the molecules are associated with each other due to the molecular dipole moment, which contributes substantially to hold the

molecules together in crystals. The hydrogen bond that exists between the hydroxyl groups of pentaborate anion and water occurs at 3353 cm^{-1}.

The B-O vibrations of borate crystals have their absorption bands from 789 cm^{-1} to 932 cm^{-1}. The strong intensity peak observed at 1082 cm^{-1} is due to ring B-O asymmetric stretching vibrations.

3.3.4.1.3 External vibrations

The external vibrations are mainly due to the bands observed below 500 cm^{-1} which are due to the rotational and translational modes of vibrations of SPB ions. The rotational modes are expected to have higher frequency and intensity than translational modes in the Raman spectra. However, the translational modes are more intense in IR spectra (Bhatacharjee 1990 and Hanuza and Fomitsev 1980). SPB is found to have 24 external modes and these vibrations can be achieved experimentally by Polarized Raman measurements. The correlation scheme for SPB is given in Table 3.3.

Table 3.3 Correlation scheme for SPB

Factor group Symmetry	Activity	
	IR	Raman
A_g	-	α_{xx}, α_{yy}, α_{zz} α_{xy}
A_u	Z	-
B_g	X,Y	α_{xz} α_{yz}
B_u	X,Y	-

3.3.5 Infra Red and Raman Spectral Analyses

Infrared spectroscopy finds application in determining the site of co-ordination, the nature of the metal-ligand bonding as well as for the elucidation of structures of co-ordination compounds (functional groups). Raman spectroscopy is an important method for investigating molecular vibrations. The exact wave number shift will depend upon the rotational and vibrational energies of the specific compound causing Raman scattering.

3.3.5.1 FT-IR spectral analysis

The FTIR spectrum of SPB crystal was recorded using KBr pellet technique in the range of 400-4000 cm^{-1} by BRUKER Model IFS 66v FT-IR spectrometer and the recorded spectrum is shown in Figure 3.6. From the molecular structure of SPB, it is clear that there is a strong molecular association, which exists due to the intermolecular hydrogen bond forces. Hence the molecule consists of BO and OH groups.

It is well known that the absorption characteristics of the crystal largely depend on the molecular bonding of the crystals. A strong molecular association exists between the molecules of SPB due to their intermolecular hydrogen bond forces. Also, there is a strong hydrogen bond force due to the hydrogen bond that exists between the hydroxyl groups of pentaborate anion and water. This molecular dipole moment contributes substantially to hold the molecules together in crystals. Further, the alkali metals have high metallic character or electropositive character, and hence their dipole absorption in IR is very strong. However sodium is less electropositive than potassium. This makes the absorption peaks to be less prominent as found with potassium, which is shown in Figure 3.6. The OH stretch of water occurs at 3353 cm^{-1}. The strong bonds observed in the IR spectrum of SPB from 789 cm^{-1} to

932 cm^{-1} have been assigned to ring B-O symmetric stretching vibrations. The ring B-O asymmetric stretching vibrations appear at 1082 cm^{-1}. The very strong peak at 1359 cm^{-1} in the IR spectra has been attributed to B-O terminal symmetric stretching vibrations.

3.3.5.2 FT-Raman spectral analysis

The FT-Raman spectrum of powdered SPB was recorded using BRUKER FRA 106 spectrometer and it is shown in Figure 3.7. The observed absorption bands along with their vibrational assignments are summarized in Table 3.4.

The strong bonds observed in the IR spectrum of SPB from 789 cm^{-1} to 932 cm^{-1} have been assigned to ring B-O symmetric stretching vibrations. In the Raman spectrum these bands appear at 776 cm^{-1} and 969 cm^{-1} respectively. The ring B-O asymmetric stretching vibrations appear at 1086 cm^{-1} and 1251 cm^{-1} with very strong intensity. The B-O terminal symmetric stretching is attributed to 1387 cm^{-1}. The B-O terminal asymmetric stretching is observed in the Raman spectrum at 1438 cm^{-1} with strong intensity.

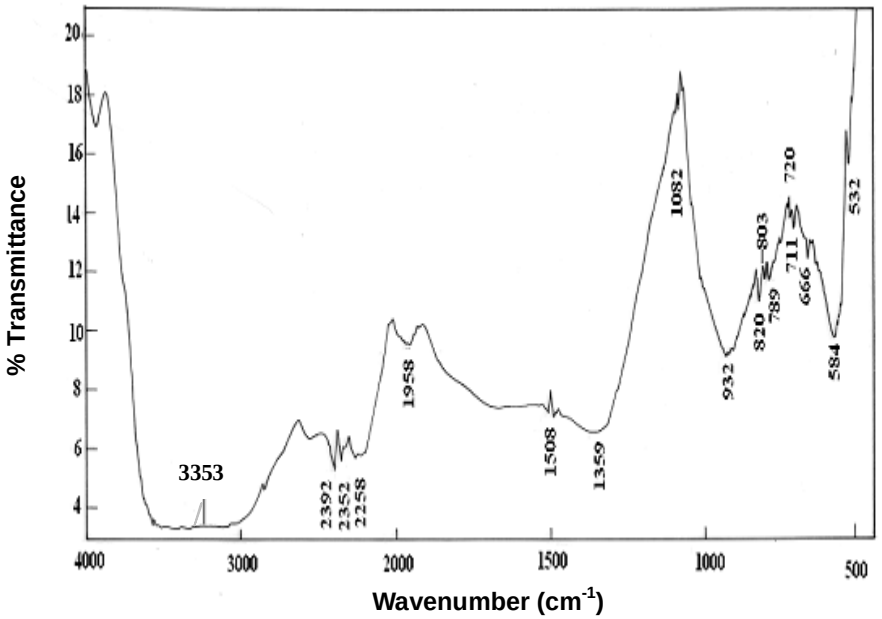

Figure 3.6 FT-IR spectrum of SPB

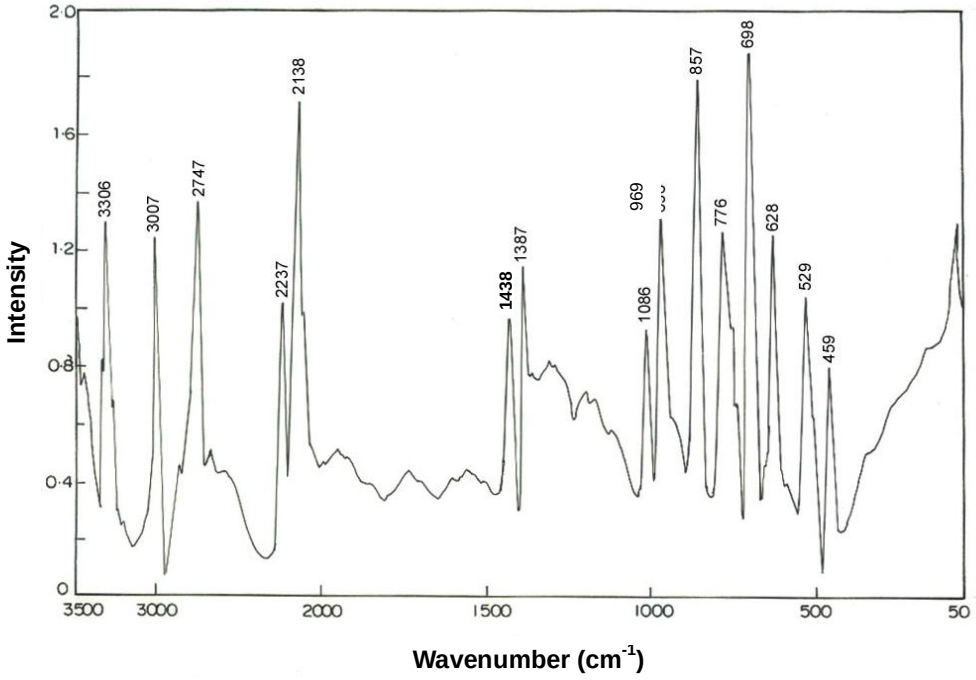

Figure 3.7 FT-Raman spectrum of SPB

Table 3.4 FT-IR and FT-Raman spectral frequencies of SPB and their assignments

Sl. No.	FT-IR (cm^{-1})	FT-Raman (cm^{-1})	Assignments
1	-	459	OBO ring bending
2	532	529	OBO terminal bending
3	666-711	628	OBO ring asymmetric bending
4	789-1082	776	B-O ring symmetric
5	820	857	B-O ring symmetric
6	932	969	B-O ring symmetric
7	1082	1086	B-O ring asymmetric
8	1359	1387	B-O terminal symmetric
9	-	1438	B-O terminal asymmetric
10	3353	-	OH stretch of water

3.4 ETCHING STUDIES OF SPB

The increasing demand for crystals of better perfection for use in the fabrication of electronic devices and in the understanding of the mechanism of plastic deformation leads to analyze the defects in crystal. Etching technique is one of the powerful tools for the observation of defects in crystals. Dislocations easily appear in the crystal especially in the initial stages of their growth (Chernov 1989). The presence of dislocations in crystal are inferred from the observation of etch pits formed (Sangwal 2005).

The as grown crystals of SPB were subjected to chemical etching studies. Water was used as etchant since it is found to be suitable for revealing dislocations. The growth features and etch patterns were observed

on the flat surface of the grown crystals. Moreover the studies were carried out at room temperature (28ºC) for a known duration ranging from 5 seconds to 15 seconds. The surface morphology of the as grown single crystals of SPB is shown in Figure 3.8.

Before etching, small etch pits are observed on the surface. The sample was then cleaned and dipped in doubly distilled water for 5, 10 and 15 seconds and dried by gently pressing between filter paper. The micro morphology was photographed and analyzed under the optical microscope. The typical etch pattern observed after etching for 5 secs in water is shown in Figure 3.8b. The etch pits are square in shape and are aligned along the flat surface. The square pattern of the etch pits (dislocation) observed is due to the high kink nucleation. The inhibitions of the etchant were high. The kink nucleation is primarily controlled by the effective undersaturation of the dissolving crystal of the etchant.

Similar etch pits with different size were observed while etching for 10 secs and 15 secs. As the etching time is increased the size of the etch pits were also found to increase but the pit pattern remains the same. This shows that etch pits or the etch patterns are dislocations outcrops at the surface. The dislocations may also be due to plastic deformation caused by thermal stresses.

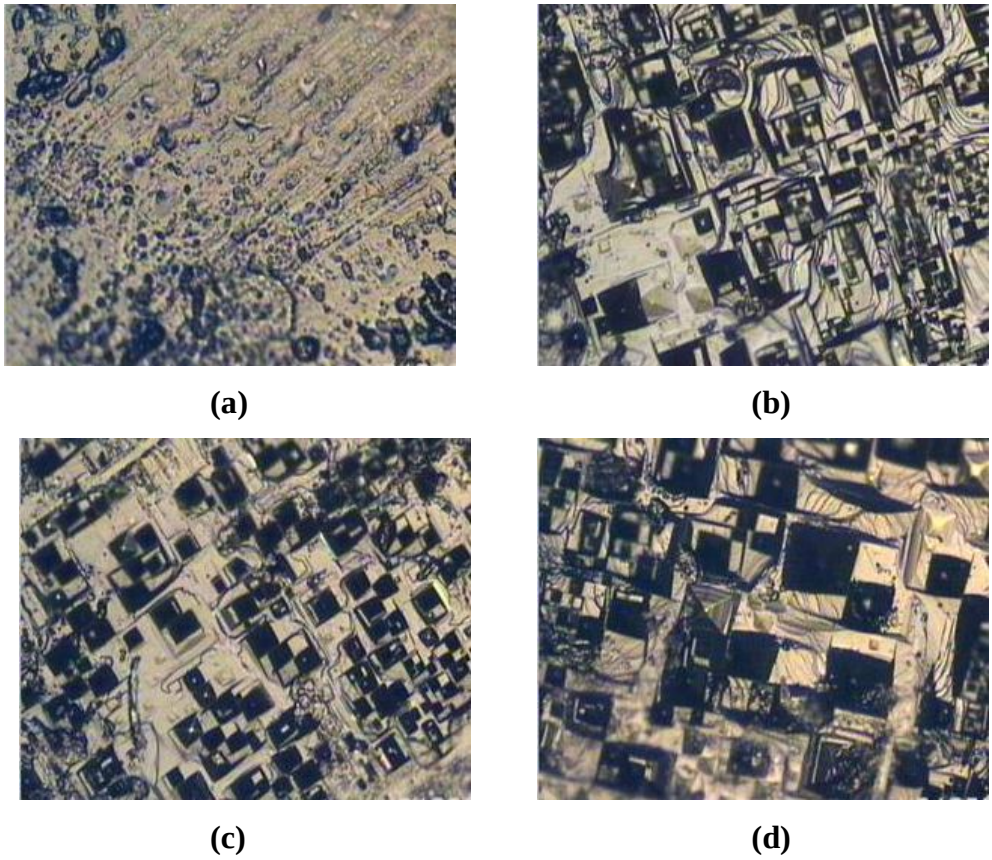

(a) **(b)**

(c) **(d)**

Figure 3.8 (a) As grown surface of SPB crystal (b), (c) & (d) etched surfaces of SPB by water for 5 sec, 10 sec and 15 sec, respectively (magnification 160 X)

The size of the etch pits on SPB become bigger with time. However their morphology in the etchant changes their size on prolonged etching time. The change in the morphology of the etch pits on prolonged etching is attributed to the time dependent adsorption of inhibiting species and solvent molecules at the newly created surface. These observations may also be associated with a decreasing undersaturation at the dislocation source with increasing time. This change in size of the etch pits can be interpreted in terms of a difference in the rate of the removal of ions from the crystal surface along different directions.

3.5 DIELECTRIC STUDIES OF SODIUM PENTABORATE

The dielectric constant is one of the basic electrical properties of solids. The measurement of dielectric constant and dielectric loss as a function of frequency and temperature is of interest both from theoretical point of view and from the applied aspects. The dielectric constant is a measure of how easily a material is polarized in an external electric field (Goma et al 2006).

The dielectric measurements of the crystal of SPB were made using HIOKI 3532 50 LCR meter from room temperature to 155^{o}C for the frequencies between 50 Hz to 5 MHz. Good quality crystals were selected and polished on a soft tissue paper with fine grade alumina powder and water. The contacts were made on either side of the sample with air drying silver paint so that it behaves as a parallel plate capacitor. The sample was housed inside a cylindrical furnace (20 cm × 20 cm × 20 cm), whose temperature is controlled by Eurotherm controller (±0.1°C).

The dielectric constant is calculated using the formula (equation 2.1) given in section 2.5. The variation of dielectric constant and dielectric loss with frequency at different temperatures is shown in Figures 3.9 and 3.10, respectively. It is found that the dielectric constant and dielectric loss increase with increasing temperature. This indicates a greater degree of lattice distortion in SPB crystals thus resulting in large proportions of space charge polarization, which ultimately causes increase of dielectric constant and dielectric loss values. The nature of variation of dielectric constant and dielectric loss with temperature in SPB is similar to alkali fluroborate (Krishna Murthy et al 2000). When the voltage is applied across the dielectric material, heat is liberated; in turn the temperature of dielectric rises and the loss increases still more.

From the plots in Figure 3.11 it can be inferred that the frequency exponent ‘s’ is independent of frequencies at all temperatures. There are various mechanisms for conduction like bond conduction, conduction in extended states, conduction in localized states near the band edge and the conduction in localized states near the Fermi level. The observed conduction in the present case can be attributed to the localized states near the Fermi level. The increase in conductivity with frequency is due to the increase in the density of energy states similar to other borates (Krishna Murthy et al 2000).

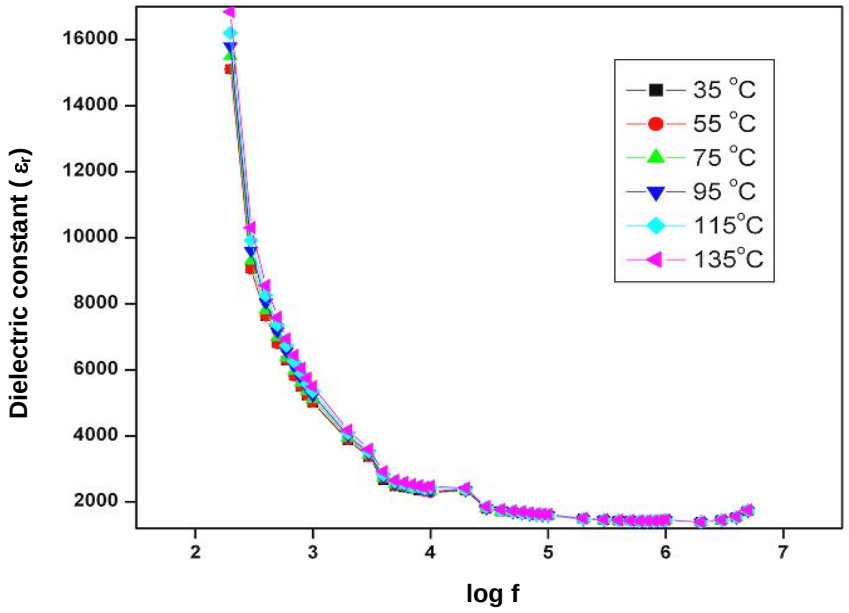

Figure 3.9 Dependence of dielectric constant of SPB with log f

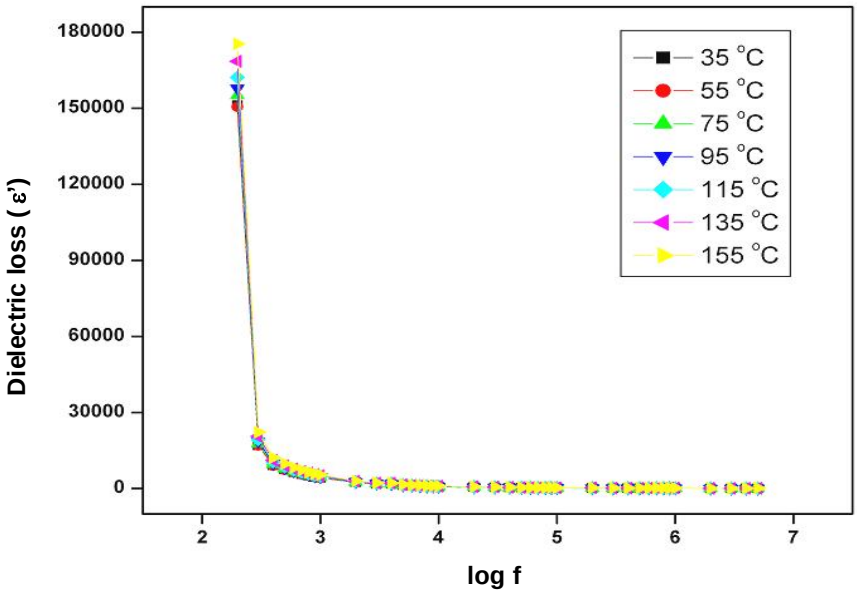

Figure 3.10 Dependence of dielectric loss of SPB with log f

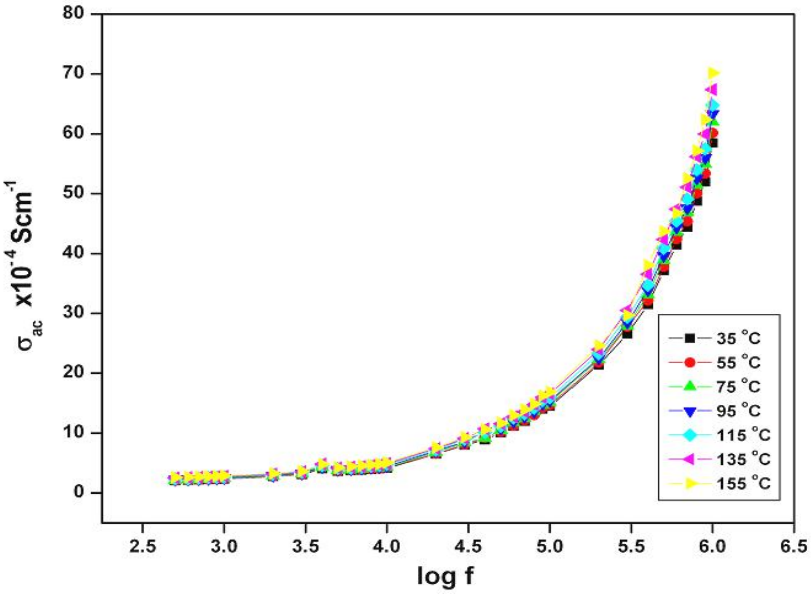

Figure 3.11 Dependence of log σ_{ac} of SPB with log f

3.6 OPTICAL PROPERTIES

3.6.1 UV-Vis. Spectral Analysis

The UV-Vis. spectral analysis gives limited information about the structure of the molecules because the absorption of UV and Visible light involves in the promotion of the electron in the σ and π orbital from the ground state to the higher energy state. For optical device applications, the wavelength range used is 1.3 to 1.5 μm in optical telecommunications since the transparency in the near IR region is significant rather than the visible region (Kaino 2000).

The UV-Vis. spectrum for SPB crystal was recorded over a wavelength range of 200-800 nm and is shown in Figure 3.12. The spectrum indicates that SPB crystal is transparent over the entire visible region and the cut off wavelength is found to be 340 nm. The optical band gap of the SPB crystal is calculated using the formula given below

$$E_g = \left(\frac{hc}{\lambda} \right) \tag{3.1}$$

The optical band gap of SPB is found to be 3.66 eV.

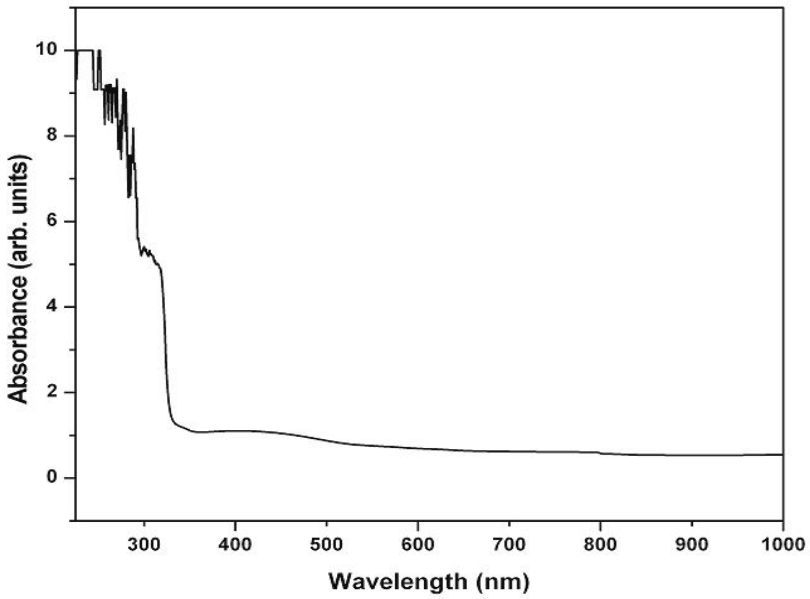

Figure 3.12 UV-Vis. Spectrum of SPB crystal

3.6.2 Theoretical Calculations of First Order Hyperpolarizability (β) of SPB

The first order hyperpolarizability value of SPB was calculated by using the GAUSSIAN 98 W and the computational details used for the calculation of β is already described in section 1.7. The first order hyperpolarizability was calculated using the Equation (1.12). All the calculations were carried out by the Density Functional triply parameter hybrid model DFT/B3LYP using GAUSSIAN 98W. The HF/3-21 G (d, p) basis set has been employed. The calculated hyperpolarizability value of SPB is 3.95×10^{-31}esu. The calculated first order hyperpolarizability (β) is presented in Table 3.5. It is found that in β_{zxx} (which is the principal dipole moment axis and parallel to the charge transfer axis) direction, the biggest values of hyperpolarizability are noticed and subsequently delocalization of electron cloud is more in that direction. This maximum value of β may be due

to the Π electron cloud movement from donor to acceptor which can make the molecule highly polarized and the intermolecular charge transfer interaction which is due to the intermolecular hydrogen bonding. The presence of intermolecular hydrogen bonding is confirmed in FT-IR analysis.

Table 3.5 First order hyperpolarizability (β) of SPB

β_{xxx}	-14.00
β_{xxy}	142.68
β_{xyy}	44.74
β_{yyy}	11.55
β_{zxx}	700.38
β_{xyz}	19.18
β_{zyy}	-336.29
β_{xzz}	-76.83
β_{yzz}	16.90
β_{zzz}	-113.87
β_{total}	3.95×10^{-31}

$\beta(-2\omega;\omega,\omega)$ in 10^{-31}esu

3.7 THERMAL PROPERTIES

The thermogravimetric (TG) and differential thermal (DT) analyzes are the suitable methods to analyze the thermal behavior since they give information regarding phase transition, water of crystallization and different stages of decomposition of the crystal (Meng et al 1998).

The thermogravimetric analysis (TGA) was carried out on the SPB crystal and the TGA spectrum was recorded at a heating rate of 2.5^{o}C/min between 100^{o}C to 800^{o}C using NETZSCH STA 409 C/CD TGA unit. The recorded TGA spectrum for SPB is shown in Figure 3.13. From the TGA spectrum it is inferred that there is 31% weight loss owing to loss of water of crystallization. One more minute weight loss was found at 566^{o}C corresponding to the condensation of defective OH grouping on the material. Figure 3.14 shows the differential thermal analysis spectrum recorded for SPB crystal. From the DTA curve it is observed that the compound is stable and there is no phase transition. However, there is an endothermic peak with maximum value of 136.7˚C, which matches with the high temperature weight loss in TGA, owing to loss of water of crystallization.

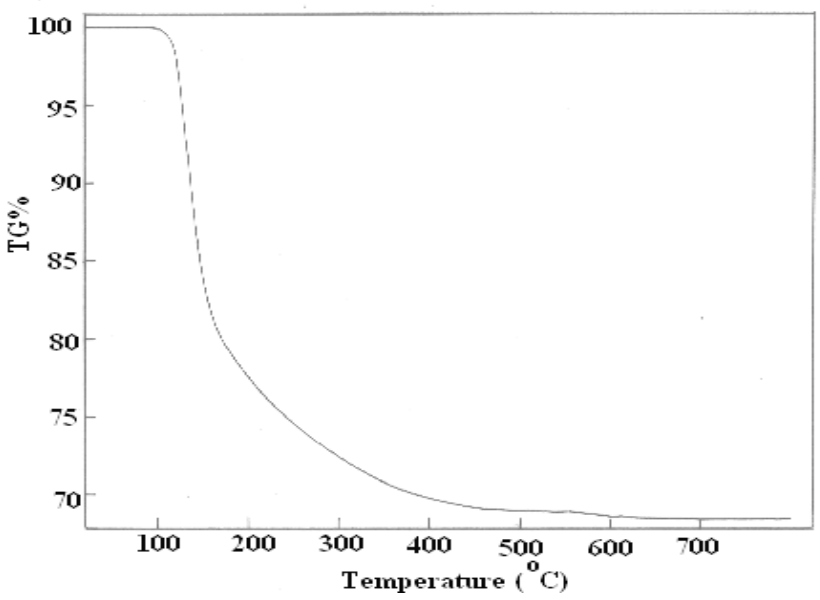

Figure 3.13 Thermogravimetric analysis of SPB crystal

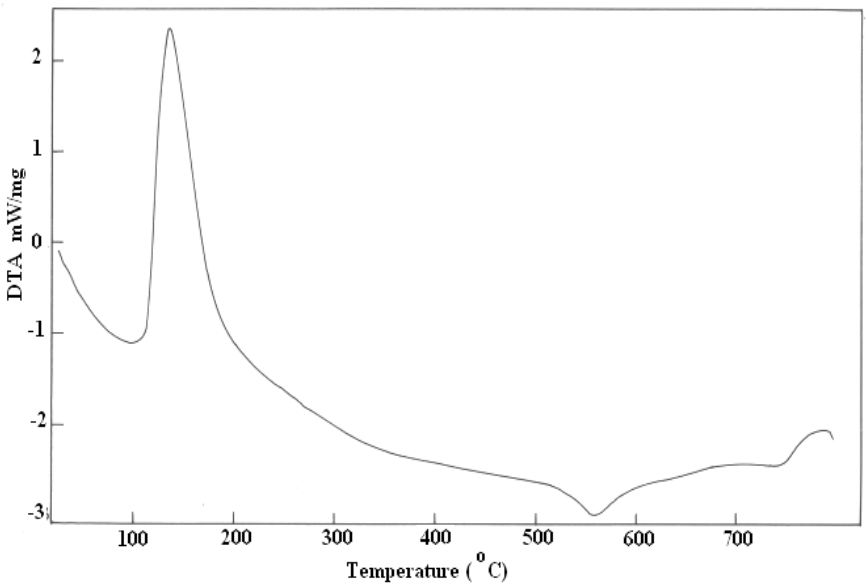

Figure 3.14 Differential thermal analysis of SPB crystal

3.8 MECHANICAL PROPERTIES

3.8.1 Microhardness Measurements

Mechanical properties of the crystalline and non-crystalline solids are intimately connected with their other physical and electrical properties and determine the performance of devices prepared from the solids. Hardness of the crystal carries information about the strength, molecular bindings, yield strength and elastic constants of the material.

The microhardness of SPB crystal was determined using the Vickers microhardness tester fitted with the diamond pyramidal indenter. During an indentation process the external work applied by the indenter is converted to a strain energy component which is proportional to the volume of the resultant impression and the surface energy component proportional to the area of the resultant impression (Gong and Ying 2000). Hence,

indentations were made on the (131) plane and microhardness measurements were made for the applied loads varying from 1 to 10 g for a dwell time of 5 s. Fine indentations were made for each load and the diagonal lengths of the indented impressions were measured. The average diagonal length of the indented impressions was calculated and the Vickers microhardness number was found from the relation

$$H_v = 2P \sin(\theta/2)/d^2 \tag{3.2}$$

If P is the average applied load (in kg), d is the average diagonal length of the indented impressions (in mm) and the angle between the opposite faces of the diamond pyramid is $\theta = 136°$, the H_v in kg/mm^2 is given by

$$H_V = 1.8544\left(\frac{P}{d^2}\right) \tag{3.3}$$

The microhardness profile as a function of applied load is shown in Figure 3.15. From the profile it is observed that the hardness value of the crystal increases with increasing applied load. This is due to the reverse indentation size effect (Mythili et al 2007). The relationship between load and size of the indentation is given by Meyer's law (Meyer 1951) $P = kd^n$, where P is load, d is diagonal length of the impression, k and n are constants for a particular material. From the slope of log P and log d plot, the value of Meyer's index number (n) was calculated. On observing this for different materials, Onitsch showed that n lies between 1 and 1.6 for hard materials and above 1.6 for soft materials (Onitsch 1947). The n value for the SPB crystal is found to be 6.1, which reveals that the grown SPB crystal is less hard in nature (Jagannathan et al 2007).

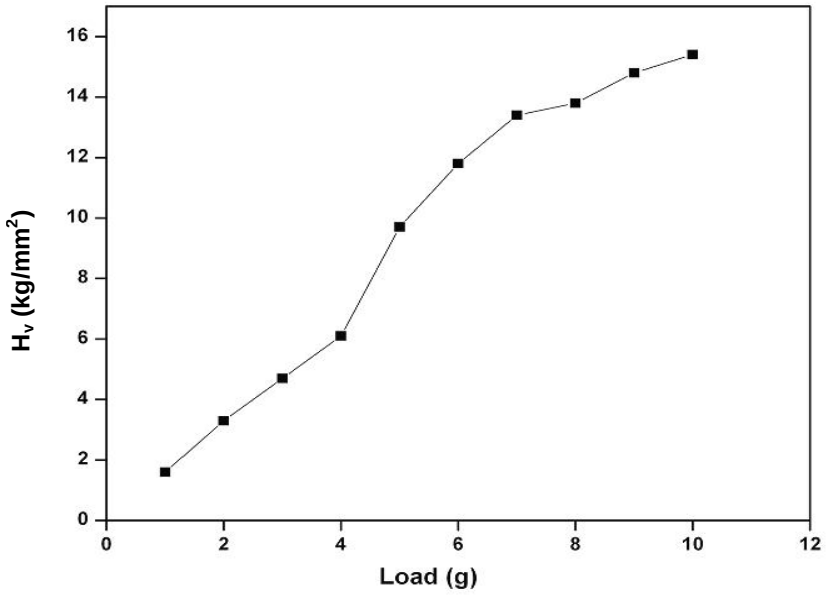

Figure 3.15 Dependence of hardness number of SPB crystal on load

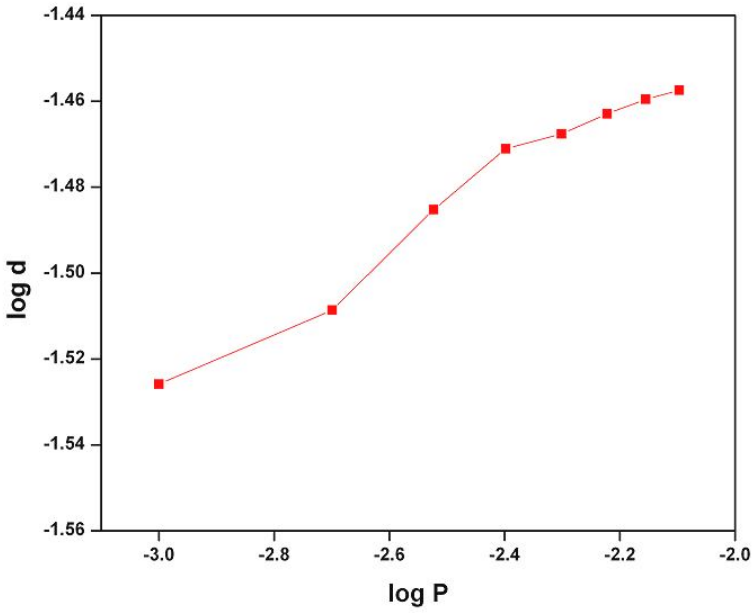

Figure 3.16 Plot of log P Vs log d of SPB crystal

3.9 CONCLUSION

The growth of single crystals of sodium pentaborate by low temperature solution growth technique is reported for the first time in the literature. Highly transparent optical quality single crystals were grown within a growth period of 40 days. The grown single crystal was subjected to single crystal X-ray diffraction studies and the lattice parameters were obtained. The morphology unveils the growth habits of the material. The structural perfection of the grown SPB was analyzed by HRXRD study. The HRXRD result elucidates the incorporation of the solvent into the growing crystal which is common in solution grown crystal and showed a very low angle boundary. The presence of the functional groups was confirmed by the FT-IR and FT-Raman spectral analyzes. Density functional theory calculations were performed for the SPB crystal to evaluate the first order hyperpolarizability value. The calculated first order hyperpolarizability of sodium pentaborate was found to be very high of the order of 3.95×10^{-31}esu. The theoretical factor group analysis of SPB predicts that there are 240 vibrational optical modes and are seen to decompose into $\Gamma_{237} = (60\ A_g + 59\ A_u + 60\ B_g + 58\ B_u)$ apart from three acoustic modes ($1A_u + 2\ B_u$).

A satisfactory study on the behaviour of the dielectric constant, dielectric loss and the conductivity of the grown SPB crystals was carried out. The variation of dielectric constant of SPB as a function of frequency indicates that the dielectric constant is higher in low frequency region and lower in the high frequency region, which substantiate that the space charge polarization predominates. Conductivity measurements show that the conduction is high at higher frequencies, which is predominantly due to the increase in the density of energy states.

The photoluminescence studies reveal the high structural perfection of the crystal as there are no additional peaks in the PL spectrum which is confirmed in the HRXRD studies. The optical properties of the grown crystal were studied using the UV-Vis. spectral analysis and the optical bandgap of the crystal is found to be 3.66 eV. The thermal properties reveal that there is no phase transition and that the material is thermally stable. The hardness studies explore the mechanical properties of the SPB crystal. The hardness number was found to increase with increasing load, which is due to the indentation size effect. The crystal was found to be less hard in nature.